Bulletin of the Seismological Society of America, Vol. 93, No. 4, pp. 1479–1497, August 2003

High-Precision Relative Locations of Two Microearthquake Clusters in Southeastern Sicily, Italy

by Luciano Scarfì, Horst Langer, and Stefano Gresta

Abstract In November 1999 and January 2000, two microearthquake swarms occurred in southeastern Sicily (Italy). They were analytically located in the depth range 17–25 km, some kilometers northward from the buried front of a regional foredeep, below the active thrust zone of the Sicily mountain chain. Their hypocentral distribution showed two distinct clusters, and comparison of the waveforms revealed clearly that the two swarms formed two distinct families of multiplet events. This led us to (1) carry out a precise relocation relative to two chosen master events of the families and (2) better define the geometrical structure of the two clusters. The cross-spectral method was applied to obtain precise readings of the wave onsets. *SH* wave onsets were used instead of *P* waves, as they showed clearer onsets and a good signal-to-noise ratio. Residuals of the relative locations showed small values, no more than several meters on average. The vertical extent of the two relocated clusters was 500 and 250 m, respectively, while the horizontal extent was 250 m. Hypocenters of the first cluster clearly delineate a north-northwest–trending plane with almost vertical dip, matching one nodal plane of the focal mechanism obtained as a composite solution of all events of the cluster. Given the considerable gap angles, because of unfavorable network geometry with respect to the events, the stability of our results was tested carrying out a Monte Carlo experiment. Varying the onset times randomly in the range of ± 5 msec, a dispersion of the locations less than 10 m in longitude and less than 50 m both in latitude and depth was found. Similar results were obtained when comparing relocations carried out with different master events. Thus, the overall geometrical characteristics of the clusters were not affected seriously by random errors.

Considering the geostructural framework of the region, together with the location and time evolution of the two clusters, fluids of plutonic origin are suggested as the trigger mechanism.

Introduction

Earthquake distribution in a given area supposedly reflects underlying tectonic patterns, such as the orientation of principal dislocations, the presence of active faults, and their relation to structures visible at the surface. The creeping segments of large fault systems, such as the San Andreas Fault, are traced by the distribution of hypocenters, and aftershock sequences are assumed to be closely related to the fault geometry of the mainshock. In this article, we deal with earthquake activity developed on a scale of a few kilometers or less. On this scale the interpretation of seismicity patterns in terms of the geometry of tectonic elements is difficult, as we have to be aware of the possibility that the distribution of hypocenters is blurred by the errors in the standard location procedures. These errors either inhibit the resolution of the geometry of the underlying tectonic elements or, even worse, may artificially create patterns that are an effect of an unfavorable station configuration or unknown velocity changes, rather than the genuine geometry of seismogenic features. Here we analyze the earthquake locations of two earthquake swarms that occurred in southeastern Sicily, considering the actual geometry of the local seismic network with respect to hypocenter locations.

Earthquakes that are characterized by very similar waveforms are named multiplets (or doublets if only two). They have been interpreted as stress release on fault asperities or clusters of asperities (Geller and Mueller, 1980; Pechmann and Kanamori, 1982). Tsujiura (1983a,b) suggested that such families of events are characteristic of earthquake swarms due to repeated slip on the same fault plane, whereas foreshock–mainshock–aftershock sequences, featuring more diverse waveforms, represent independent ruptures in a complex fault zone.

These events have been associated with both tectonic (e.g., Poupinet *et al.*, 1984; Ito, 1985; Scherbaum and Wendler, 1986; Console and Di Giovambattista, 1987) and volcanic activity (e.g., Frémont and Malone, 1987; Got *et al.*, 1994). Multiplets have also been used to measure time variations of crustal parameters with high precision (Frémont, 1984; Fréchet, 1985; Poupinet *et al.*, 1985) and for the imaging of tectonic structures of small extent (Deichmann and Garcia-Fernandez, 1992). The location of earthquake families relative to master events can be carried out with high precision, under favorable conditions to an accuracy of a few meters, which allows us to investigate small tectonic features (e.g., Rowe *et al.*, 2002) and/or accurate time migration of foci in near real time (e.g., Phillips, 2000; Got *et al.*, 2002).

In relative location procedures, one focuses on spatial offsets between earthquake hypocenters rather than their absolute position. If the hypocentral separation between two earthquakes is small compared to the event–station distance, then the ray paths between the source region and a common receiver can be assumed to be similar along almost the entire path of the ray. In this case, travel-time differences can be attributed to the spatial offset between the two events, whereas the absolute errors are of common origin except in the region where the ray paths differ at the sources. Thus the scatter of relative hypocenter clusters is considerably reduced with respect to absolute locations. Recently, Waldhauser and Ellsworth (2000) introduced a double difference relative location algorithm that can be applied both to multiplet and nonmultiplet events. Their method inverts for all relative travel-time differences, in effect treating every member earthquake as a master event and finding a consistent master–slave relationship for a complete catalog in terms of relative hypocenter locations. The approach, however, is stable only with a sufficient number of travel-time readings and a favorable station configuration (e.g., Ross *et al.*, 2001).

Here we investigate the origin of two microearthquake swarms in southeastern Sicily. In a previous article, Scarfì *et al.* (2001) have shown that the two swarms form two families of multiplets. The geometry of the earthquake clusters is analyzed using relative locations based on a master-event technique. First, we review the various pieces of evidence for the existence of two distinct families by comparing waveforms, analyzing the relation of *P*- and *S*-wave amplitudes and carrying out composite fault-plane solutions. Then, on the basis of these findings, we identify master events by selecting the events that showed high cross-correlation coefficients with the greatest number of events belonging to a family.

The relocation of multiplet events is based on accurate determination of the time differences *dt* of *P* or *S* phases for different events at the same stations. Concerning the accuracy of time-difference determination, we take into account arrival-time quality, which is of the order of milliseconds. Among possible sources of time errors we essentially avoid problems of noisy data by using *SH* waves instead of *P* waves. However, small instrumental errors of time resolution may have escaped the attention of the analysts, and (similar to the absolute locations) the configuration of the seismic network with respect to the hypocenters may introduce biases in the inferred geometry of the earthquake clusters. We therefore check our relocation results by Monte Carlo experiments, wherein we introduce random perturbations to the phase differences and analyze the scatter of the solutions. A comparison of the originally obtained residuals in the relocation with those obtained using "noisy" time differences gives us a rough idea about the upper limit of a possible undiscovered inaccuracy of time resolution. We verify the conclusions drawn from the Monte Carlo experiment by exchanging the master events and comparing the obtained relative positions of the earthquake family members.

Finally, the distribution of foci within the two accurately relocated clusters is discussed in terms of both the regional geostructural framework and possible earthquake-triggering mechanisms.

Structural and Seismic Features of the Area

Eastern Sicily is characterized by a complex tectonic setting in the frame of the collisional process affecting the African–European convergent belt. The overall structure of this active zone is made up, from north to south, of three main structural units: the active thrust belt (Northern Chain), the Gela–Catania foredeep, and the Hyblean Plateau (Lentini *et al.*, 1994; see Fig. 1). The Hyblean area is considered to be part of the northern margin of the African plate that remained as a relatively undeformed foreland during the Neogene collisional process. It is bounded (Fig. 1) to the east by a north-northwest–south-southeast–trending lithospheric fault system, the morphological evidence of which is the Malta escarpment. It separates the Sicilian foreland from the oceanic crust in the Ionian Sea (Scandone *et al.*, 1981; Ben-Avraham *et al.*, 1995; Hirn *et al.*, 1997). Another main fault system of the Hyblean Plateau is the "Scicli–Ragusa–Mt. Lauro line" zone (Fig. 1). Following Grasso and Reuther (1988) this lineament forms a strike-slip fault zone developing over a length of about 100 km from the Sicily Straits to the northern margin of the plateau. The whole system consists of three main right-lateral fault segments, trending north–south, and of second-order structures with northeast–southwest, en échelon arrangement that accommodate the shear deformation (Ghisetti and Vezzani, 1980). These faults can be viewed as secondary structures; however, they form a complex field of horsts and grabens whose strike direction is about northeast–southwest. Moreover, they are seismogenic (Azzaro and Barbano, 2000), and they played an active role (Grasso and Reuther, 1988; Pedley and Grasso, 1991) in the magmatism and volcanism that affected the northern Hyblean margin from late Miocene to early Pleistocene (Scribano, 1987). To the north, in the Gela–Catania foredeep, the margin of the Hyblean Plateau is down-bent by the northeast–southwest fault system under the front of the Sicilian mountain chain, which is part of the

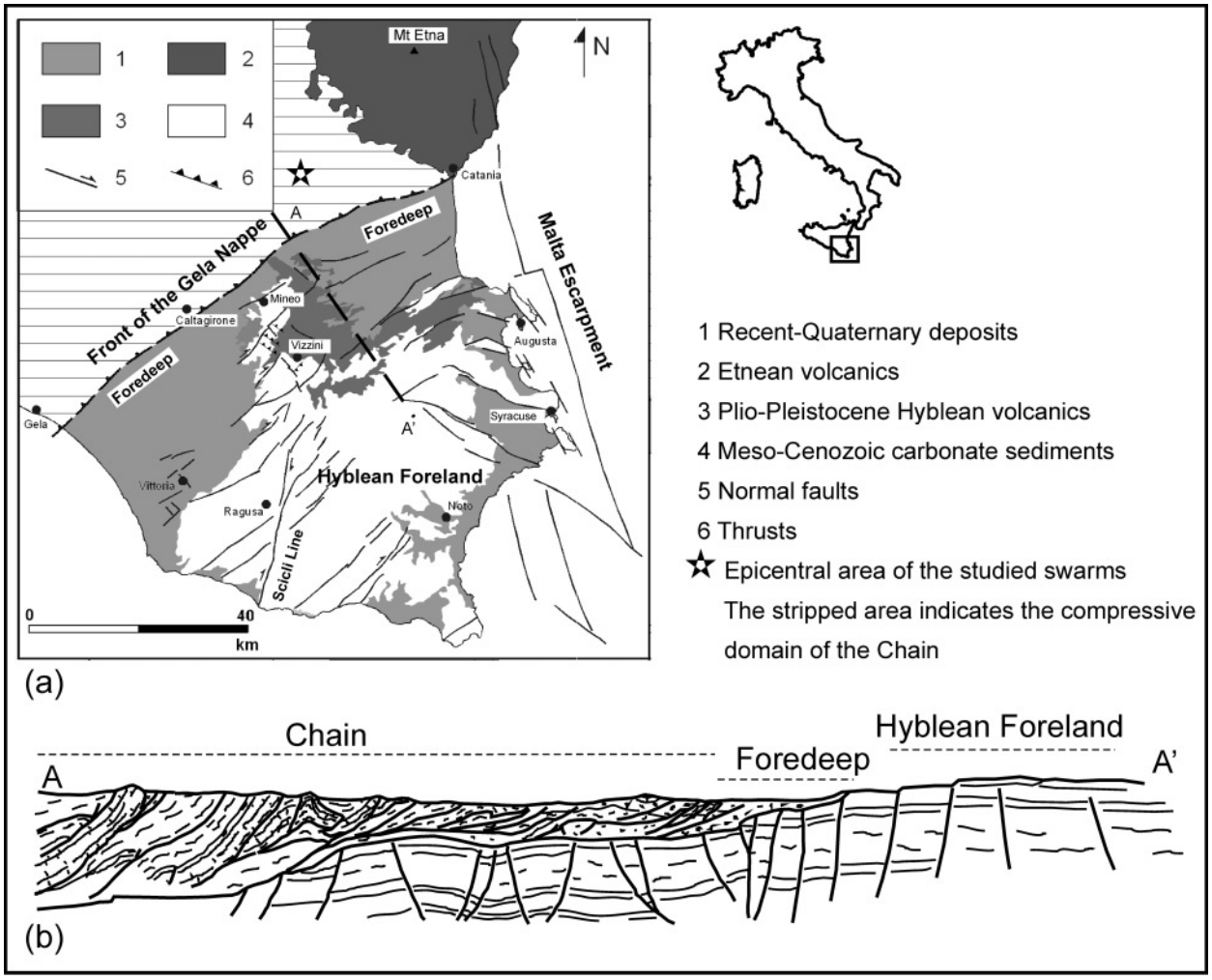

Figure 1. (a) Simplified geologic map and (b) shallow (5 km) structural section of southeastern Sicily. (Modified from Azzaro and Barbano, 2000).

Appennine–Maghrebian chain (Cogan *et al.*, 1989; Yellin-Dror *et al.*, 1997).

The definition of seismogenic sources in this region has been the subject of intense discussion (e.g., Bianca *et al.*, 1999; Sirovich and Pettenati, 1999; Barbano and Rigano, 2001) due principally to the few instrumentally recorded earthquakes. The distribution of major historical earthquakes (Fig. 2) gives no clear evidence for the identification of dominant active seismic structures. Consequently, no unique interpretation has so far been accepted. Among the earthquakes occurring in the time span from the ninth century until the present, the largest (macroseismic magnitude ca. 7–7.5) earthquake in southeastern Sicily occurred on 11 January 1693 (e.g., Azzaro and Barbano, 2000), causing the destruction of many cities. In spite of considerable research efforts devoted to this earthquake, its location and its possible relationship to tectonic structures are still unclear. The other main event (macroseismic magnitude ca. 7) hit the region on 4 February 1169. More recently, the shock on 13 December 1990 (M_S 5.4) caused severe damage at a local scale. Instrumental local recordings for this seismogenic area have become available only since this last earthquake, whose mechanism was an almost pure strike slip, with either left-lateral motion on a north–south vertical plane or right-lateral motion on an east–west, 62° N–dipping plane (Amato *et al.*, 1995).

The data we present here concern earthquakes occurring the site of Ramacca, close to the thrust border between the Gela–Catania foredeep and the nappes of the Northern Chain. The only significant seismic event that has occurred in the neighborhood of Ramacca is the shock on 23 December 1959 with a macroseismic epicenter about 10 km from the earthquake swarms analyzed here. This earthquake produced slight damage over an area about 60 km long, striking northeast–southwest. In spite of its moderate magnitude (M 4.7), it was well felt throughout Sicily, indicating a focal depth of some tens of kilometers (Azzaro and Barbano, 2000).

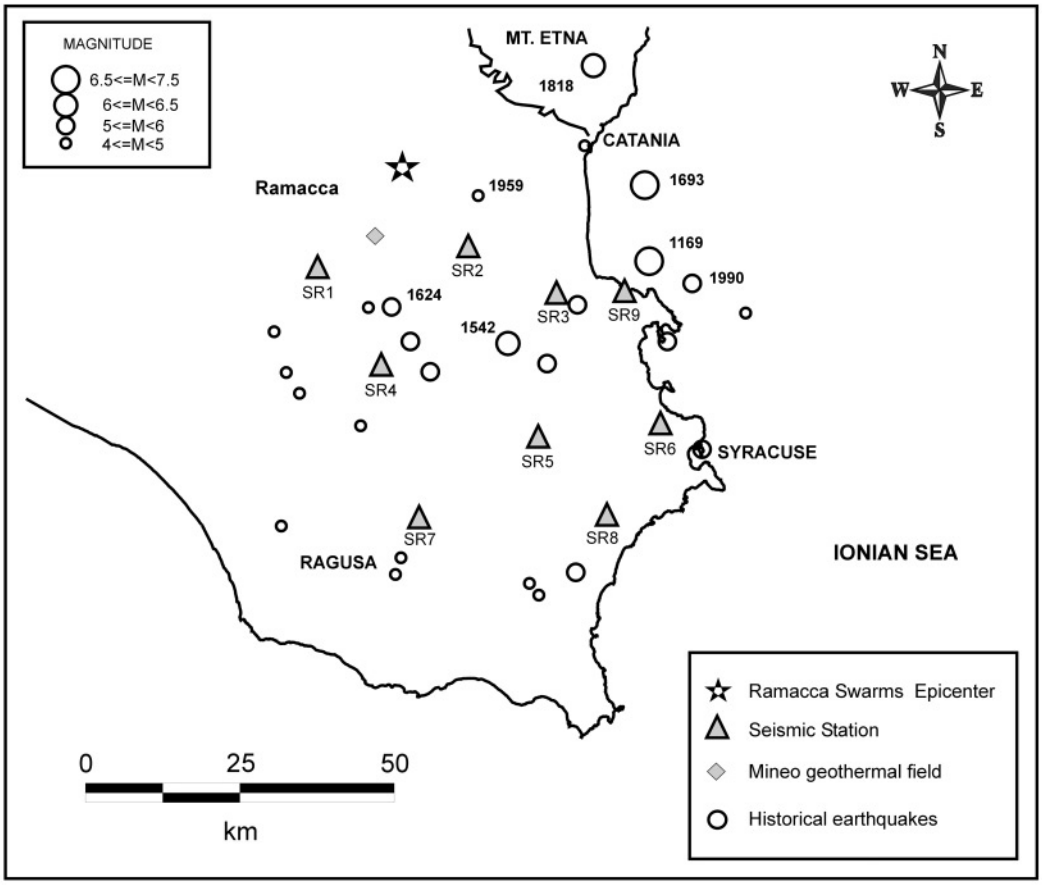

Figure 2. Map of the permanent Southeastern Sicily Seismic Network (SESSN) and of the historical seismicity (Azzaro and Barbano, 2000).

The Data

The Southeastern Sicily Seismic Network (SESSN; see Fig. 2) has been operating since 1994. It consists of nine digital three-component stations, each equipped with short-period Mark L4-3D seismometers having a natural frequency of 1.5 Hz and a damping about 60% of critical. The seismic signals are sampled at a frequency of 125 Hz and transmitted by radio telemetry to the data acquisition center in Catania. The corner frequency of the antialias filter is 51 Hz, and the amplitude resolution is formally 24 bits.

Our data set consists of 57 microearthquakes with local magnitudes (M_L) ranging from 0.7 to 2.5 (Table 1). Essentially two swarms occurred: the first in November 1999 and the second in January 2000 (Fig. 3). The first swarm of 16 events was recorded on 19 and 20 November 1999. The latter one (37 events) occurred on 1 and 2 January 2000. Isolated earthquakes followed on 3, 4, and 24 January.

Radiated seismic energy was estimated using Richter's (1958) empirical formula:

$$\log E = 9.9 + 1.9M_L - 0.024{M_L}^2,$$

where E is the energy expressed in joules and M_L is the local magnitude. Figure 3 shows the seismic energy radiated from each event, expressed as a percentage of the total energy released during the two swarms. About 88% of the total energy was released by only 11 earthquakes. These correspond to earthquakes with magnitude above 1.6, six of which occurred during the swarm of November 1999 and four on the first days of January 2000. After a period of quiescence of almost 3 weeks, the sequence finished with two events on 24 January, the second having a magnitude of 2.5. On the whole, the data set corresponds to the characteristics of earthquake swarms rather than sequences, as there is no mainshock–aftershock relation.

Earthquakes in this study have been located using the recently proposed minimum 1D velocity model for the Hyblean area, which consists of six layers and reduces both residuals and errors of the location (Musumeci *et al.*, 2003). The locations are shown in Figure 4. They differ slightly (in the order of the standard location error) from the ones previously obtained by Scarfì *et al.* (2001), who had used a more general four-layer velocity model. The events occurred within the crystalline basement, below the thrust zone (Ragg *et al.*, 1999), close to the border of the Gela–Catania foredeep.

Table 1
Earthquakes Analyzed in This Study, Their Locations and Their Relative Parameters

ID	Date	Origin time	Latitude	Longitude	Depth	M_L	rms	ERZ	ERH
1	1999/11/19	02:46:50.88	37.465	14.746	18.2	1.5	0.10	1.4	1.9
2	1999/11/19	02:48:00.53	37.467	14.746	17.7	1.0	0.09	1.3	2.0
3	1999/11/19	04:33:15.06	37.461	14.744	19.1	2.3	0.08	0.7	1.0
4	1999/11/19	04:35:38.46	37.460	14.745	18.5	1.1	0.09	0.7	1.3
5	1999/11/19	05:22:43.41	37.456	14.744	19.4	2.3	0.08	0.7	1.0
6	1999/11/19	05:51:32.19	37.456	14.746	18.6	1.0	0.07	0.7	1.3
7	1999/11/19	06:09:28.46	37.460	14.745	18.6	1.7	0.09	0.7	1.2
8	**1999/11/19**	**06:26:45.24**	**37.460**	**14.746**	**18.1**	**2.0**	**0.10**	**0.6**	**0.7**
9	1999/11/19	06:33:18.31	37.459	14.746	17.8	1.5	0.06	0.7	0.9
10	1999/11/19	06:50:41.26	37.460	14.743	19.1	1.5	0.05	0.9	1.5
11	1999/11/19	07:44:05.20	37.460	14.745	18.3	1.5	0.09	0.7	1.3
12	1999/11/19	11:47:25.41	37.468	14.747	18.1	1.3	0.10	1.4	2.2
13	1999/11/19	13:00:37.67	37.461	14.744	18.8	2.3	0.09	0.7	1.0
14	1999/11/19	13:04:47.45	37.459	14.744	18.9	1.9	0.09	0.7	1.3
15	1999/11/19	16:38:13.45	37.443	14.742	20.2	1.4	0.06	2.1	2.0
16	1999/11/20	05:57:42.35	37.470	14.747	16.9	2.0	0.10	1.2	1.3
17	*2000/01/01*	*04:02:00.27*	*37.473*	*14.736*	*23.2*	*0.9*	*0.04*	*2.6*	*3.0*
18	*2000/01/01*	*04:02:46.77*	*37.483*	*14.738*	*21.6*	*1.4*	*0.03*	*0.8*	*1.6*
19	*2000/01/01*	*04:03:18.55*	*37.482*	*14.740*	*21.6*	*1.4*	*0.04*	*0.8*	*1.6*
20	*2000/01/01*	*04:04:27.24*	*37.482*	*14.740*	*21.5*	*1.5*	*0.04*	*0.8*	*1.6*
21	*2000/01/01*	*04:07:13.07*	*37.497*	*14.744*	*19.6*	*0.9*	*0.05*	*3.4*	*4.7*
22	*2000/01/01*	*04:08:54.04*	*37.481*	*14.740*	*21.6*	*1.1*	*0.04*	*0.8*	*1.8*
23	*2000/01/01*	*04:11:24.10*	*37.483*	*14.737*	*21.6*	*1.5*	*0.04*	*0.8*	*1.6*
24	*2000/01/01*	*04:15:02.11*	*37.482*	*14.739*	*21.4*	*1.3*	*0.04*	*0.8*	*1.8*
25	*2000/01/01*	*04:15:51.96*	*37.482*	*14.739*	*21.7*	*1.4*	*0.04*	*0.8*	*1.8*
26	*2000/01/01*	*04:19:16.84*	*37.482*	*14.739*	*21.6*	*1.0*	*0.04*	*2.3*	*3.1*
27	*2000/01/01*	*04:22:39.29*	*37.481*	*14.739*	*21.5*	*2.1*	*0.04*	*0.8*	*1.6*
28	*2000/01/01*	*04:25:07.19*	*37.483*	*14.739*	*21.5*	*1.4*	*0.04*	*0.8*	*1.6*
29	*2000/01/01*	*05:06:33.20*	*37.483*	*14.738*	*21.7*	*1.6*	*0.03*	*0.8*	*1.6*
30	*2000/01/01*	*05:41:01.93*	*37.486*	*14.735*	*22.9*	*1.4*	*0.07*	*0.9*	*1.6*
31	*2000/01/01*	*05:41:18.35*	*37.481*	*14.739*	*21.5*	*1.4*	*0.03*	*0.8*	*1.6*
32	*2000/01/01*	*05:42:23.54*	*37.483*	*14.739*	*21.7*	*1.3*	*0.04*	*0.8*	*1.9*
33	*2000/01/01*	*05:58:58.30*	*37.484*	*14.740*	*21.5*	*0.9*	*0.04*	*0.8*	*1.9*
34	*2000/01/01*	*06:22:06.30*	*37.482*	*14.739*	*21.6*	*1.0*	*0.04*	*2.3*	*3.1*
35	*2000/01/01*	*07:11:03.43*	*37.483*	*14.738*	*21.7*	*0.9*	*0.04*	*2.6*	*3.2*
36	*2000/01/01*	*07:13:01.65*	*37.483*	*14.737*	*21.5*	*1.9*	*0.04*	*0.8*	*1.6*
37	*2000/01/01*	*08:15:18.17*	*37.482*	*14.739*	*21.2*	*0.9*	*0.03*	*0.8*	*1.9*
38	*2000/01/01*	*09:57:08.10*	*37.437*	*14.744*	*25.3*	*0.8*	*0.04*	*10.5*	*5.9*
39	*2000/01/01*	*10:02:21.18*	*37.464*	*14.733*	*21.6*	*1.6*	*0.02*	*2.8*	*3.0*
40	*2000/01/01*	*10:03:02.87*	*37.481*	*14.739*	*21.7*	*1.7*	*0.03*	*0.8*	*1.6*
41	*2000/01/01*	*10:27:54.01*	*37.484*	*14.740*	*20.8*	*1.2*	*0.04*	*0.8*	*1.1*
42	*2000/01/01*	*10:33:45.81*	*37.485*	*14.741*	*20.9*	*0.9*	*0.04*	*1.8*	*1.7*
43	*2000/01/01*	*10:35:54.34*	*37.485*	*14.741*	*20.6*	*0.8*	*0.04*	*1.7*	*1.7*
44	*2000/01/01*	*23:00:15.09*	*37.484*	*14.740*	*21.1*	*1.3*	*0.05*	*2.2*	*2.8*
45	*2000/01/01*	*23:02:10.10*	*37.458*	*14.734*	*24.8*	*1.5*	*0.02*	*3.3*	*3.5*
46	*2000/01/02*	*07:20:28.81*	*37.481*	*14.744*	*20.1*	*0.9*	*0.01*	*2.1*	*3.1*
47	*2000/01/02*	*07:36:30.24*	*37.483*	*14.739*	*21.7*	*1.4*	*0.04*	*0.8*	*1.6*
48	*2000/01/02*	*07:53:43.72*	*37.484*	*14.739*	*21.6*	*1.8*	*0.04*	*0.8*	*1.6*
49	*2000/01/02*	*08:04:53.51*	*37.483*	*14.739*	*21.5*	*1.5*	*0.04*	*0.8*	*1.6*
50	*2000/01/02*	*08:38:08.84*	*37.482*	*14.739*	*21.6*	*1.4*	*0.04*	*0.8*	*1.6*
51	***2000/01/02***	***09:24:40.27***	***37.483***	***14.741***	***21.1***	***2.0***	***0.05***	***0.8***	***1.3***
52	*2000/01/02*	*10:28:38.02*	*37.482*	*14.739*	*21.6*	*1.3*	*0.04*	*0.8*	*1.6*
53	*2000/01/02*	*12:07:47.21*	*37.481*	*14.740*	*20.4*	*1.6*	*0.06*	*0.8*	*1.3*
54	*2000/01/03*	*04:28:18.58*	*37.482*	*14.740*	*21.4*	*0.7*	*0.04*	*2.3*	*3.2*
55	*2000/01/04*	*19:42:55.56*	*37.483*	*14.737*	*21.5*	*1.4*	*0.04*	*0.8*	*1.6*
56	*2000/01/24*	*15:51:46.69*	*37.441*	*14.743*	*20.8*	*1.1*	*0.06*	*2.2*	*2.4*
57	*2000/01/24*	*16:38:08.45*	*37.455*	*14.746*	*18.9*	*2.5*	*0.07*	*0.9*	*1.1*

Master events are indicated in bold type, events belonging to family 2 in italics. ERZ and ERH are the standard location errors in the horizontal and vertical direction, respectively.

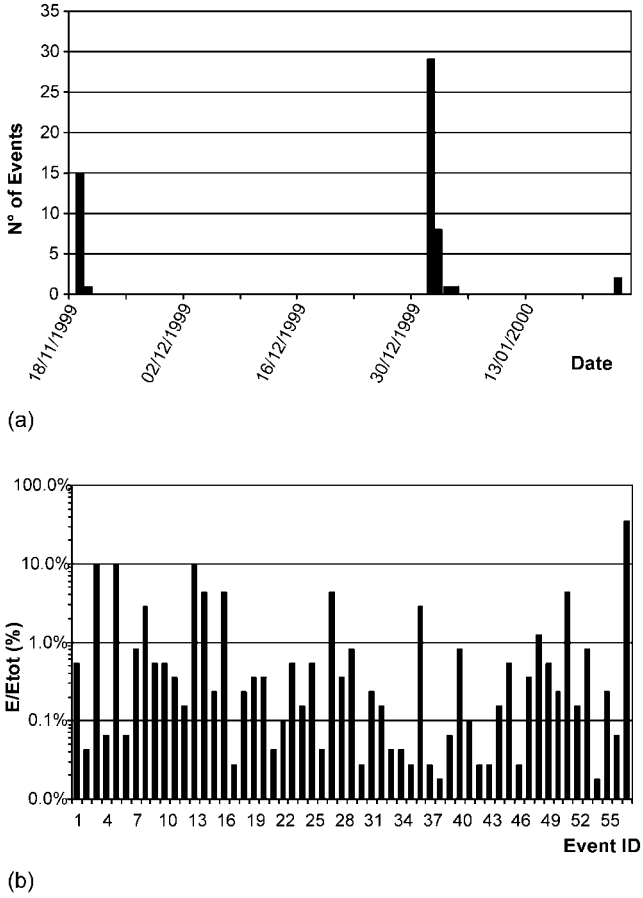

Figure 3. (a) Earthquake time distribution; (b) relative radiated seismic energy by the single event. 100% corresponds to the total energy released during the two swarms.

The Identification of Earthquake Families

A crude visual inspection revealed strong similarities of waveforms among many events (Fig. 5). As a simple measure of similarity Scarfì *et al.* (2001) used the maximum of the cross-correlation function between the vertical component seismograms, using time windows of 8 sec starting from the first *P*-wave onset. They calculated the matrix of maximum cross-correlation coefficients for all events reported in Table 1 The data set represented in the matrix was arranged according to the chronological sequence with the exception of the events of 24 January 2000. For the sake of clarity these events were put on the tail of the ones of November 1999. The matrix of the cross-correlation coefficients is graphically visualized in Figure 6 for station SR1. Similar results were obtained for matrices of stations SR2 and SR3. From the graph we identify clearly two rectangular areas where high cross-correlation coefficients occur. These indicate two distinct groups, since high correlation coefficients are observed only inside the two rectangular areas, that is, only among records that belong to the same families.

Scarfì *et al.* (2001) compared the relation of vertical component *P*-wave peak amplitudes and maximum horizontal peak *S*-wave amplitudes. At all three key stations the *P*/*S*-wave amplitude ratios of the events that occurred in November 1999 differ significantly from those of January 2000. As already noted for the cross-correlation coefficients, the events of 24 January show the same features as the events belonging to the cluster of November 1999 (Fig. 7).

Grid Search Location

Looking at the picture of standard locations (Fig. 4), the epicenters appear to align on north–south–trending planes with an almost vertical dip. However, the characteristics of the two Ramacca swarms as multiplet events raise serious questions as to the picture obtained from the standard location procedures, because the high degree of similarity among multiplet events strongly suggests that the earthquakes form clusters of small extent. On the other hand, the apparent extent of the clusters inferred from the absolute locations corresponds to about twice its error (of the standard location) both in horizontal and vertical coordinates. Thus we suspect that the geometry of the hypocenter clusters may be an artifact introduced by the nonoptimal network configuration with respect to the position of the foci, and the estimated errors may be too small.

We examined the resolution capability of the SESSN with respect to the Ramacca swarms, carrying out a grid search location for selected events. For this purpose we defined a 3D grid of points in a cube having 5-km sides surrounding the hypocenter of each of the examined earthquakes. With a spacing of 150 m horizontally and 300 m vertically, we obtain a total of 16,660 points, for which we calculated theoretical travel times for *P* and *S* waves. Comparing these with the observed times, we constructed a cube of the root mean square (rms) travel-time residuals obtained for each of the 16,660 points. The point with the lowest residuals is identified as the global optimum, whereas the spatial distribution of the residuals yields a measure for the stability of the location. Extended areas with low rms values indicate an unstable solution, whereas narrow minima represent stable solutions.

In Figure 8 we have plotted three cross sections of the rms residuals cube obtained for event 1. The cross sections are oriented parallel to the Earth's surface, vertically in the east–west and north–south directions, respectively. All cross sections are centered with respect to the global minimum. In Figure 8 we immediately recognize a north–south–trending zone with residuals of 0.1 sec or below, extending for about 1.5 km. In the vertical cross sections the minima define an 80° W–dipping plane, with an extension of about 2 km. In north–south direction we note an inclination of the minimum area of about 45°. Figure 8 is representative of all examples examined with the grid search location. It resembles strongly the shape of the clusters identified by the standard location and confirms our hypothesis inferred from the similarity of

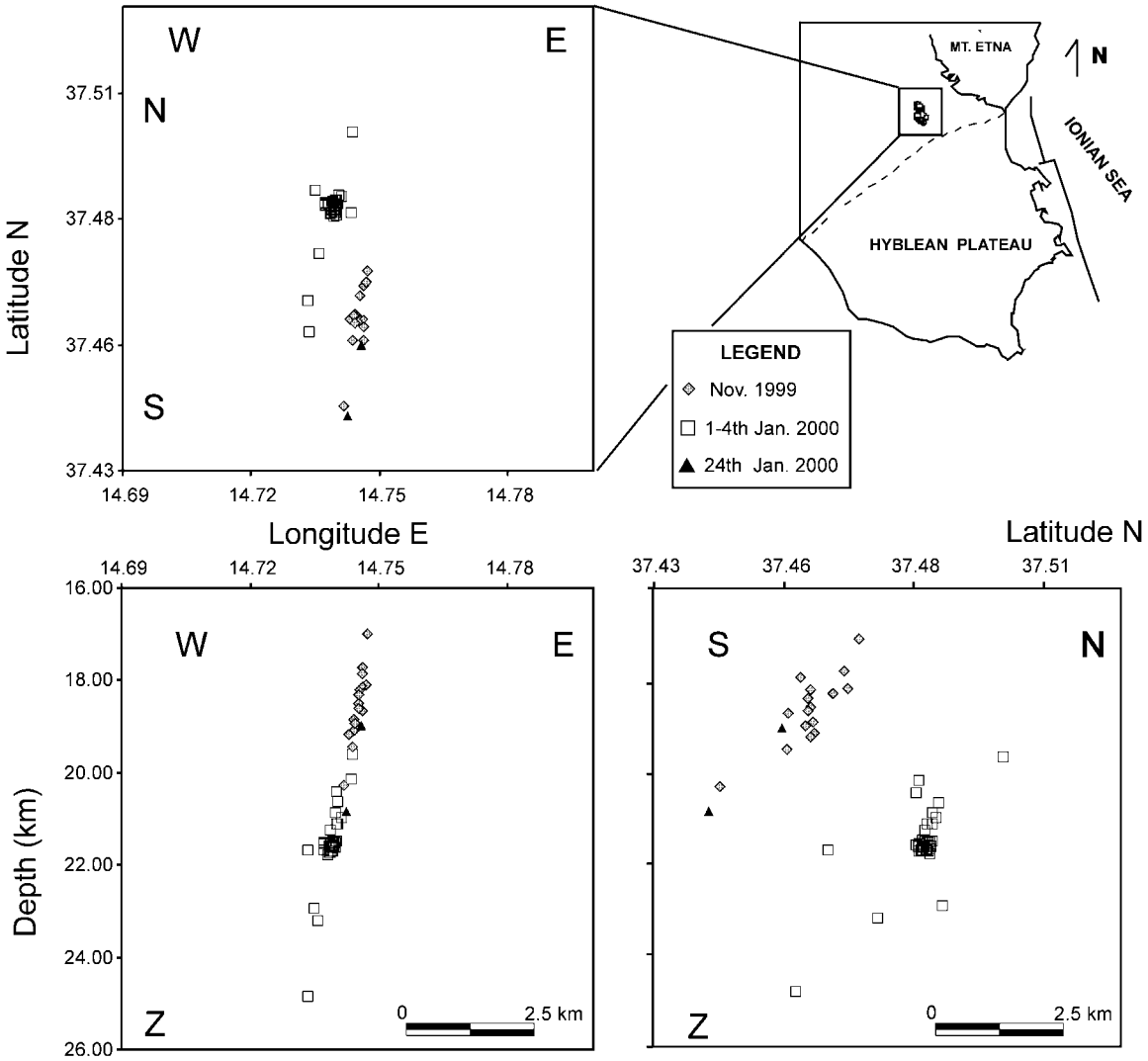

Figure 4. Epicentral map (top right) and hypocentral distribution of the whole seismic sequence, as inferred from absolute locations. Different symbols correspond to various time periods of occurrence (see the legend).

the waveforms: that the hypocenters may be indeed situated very closely together.

Multiplet Analysis

It is common knowledge that relative location procedures of multiplet events yield an accuracy far above those from absolute locations (e.g., Poupinet *et al.*, 1984). The general strategy of relative location is to determine accurately the time differences *dt* of phases for different events at the same stations and to locate the position of a "slave" earthquake relative to a reference "master" event. In effect, if both the slave and the master event were located exactly at the same place, the time differences *dt* would be the same at all stations and equal to the difference in origin times of the two events, regardless of the absolute location uncertainties.

A key problem of high-precision location is arrival-time picking. Two methods that are commonly used, the cross-correlation method (Deichmann and Garcia-Fernandez, 1992) and the cross-spectral method (Poupinet *et al.*, 1984; Frémont and Malone, 1987), point to the moment centroid. In other words, they focus on the position of the part of the fault radiating the most energy, rather than the first break, which corresponds to the point where rupture begins. First onset readings are based on the time when the first deviation of the trace from the background occurs. The actual achievable time accuracy is thus also a function of the sharpness of the signal in relation to noise level and is limited by the sampling rate. On the other hand, as the position of the moment centroid is determined from a window of finite length, a resolution finer than the sampling rate can be achieved. This also implies that relative earthquake locations may differ less than individual source diameters, that is, overlapping sources may be identified.

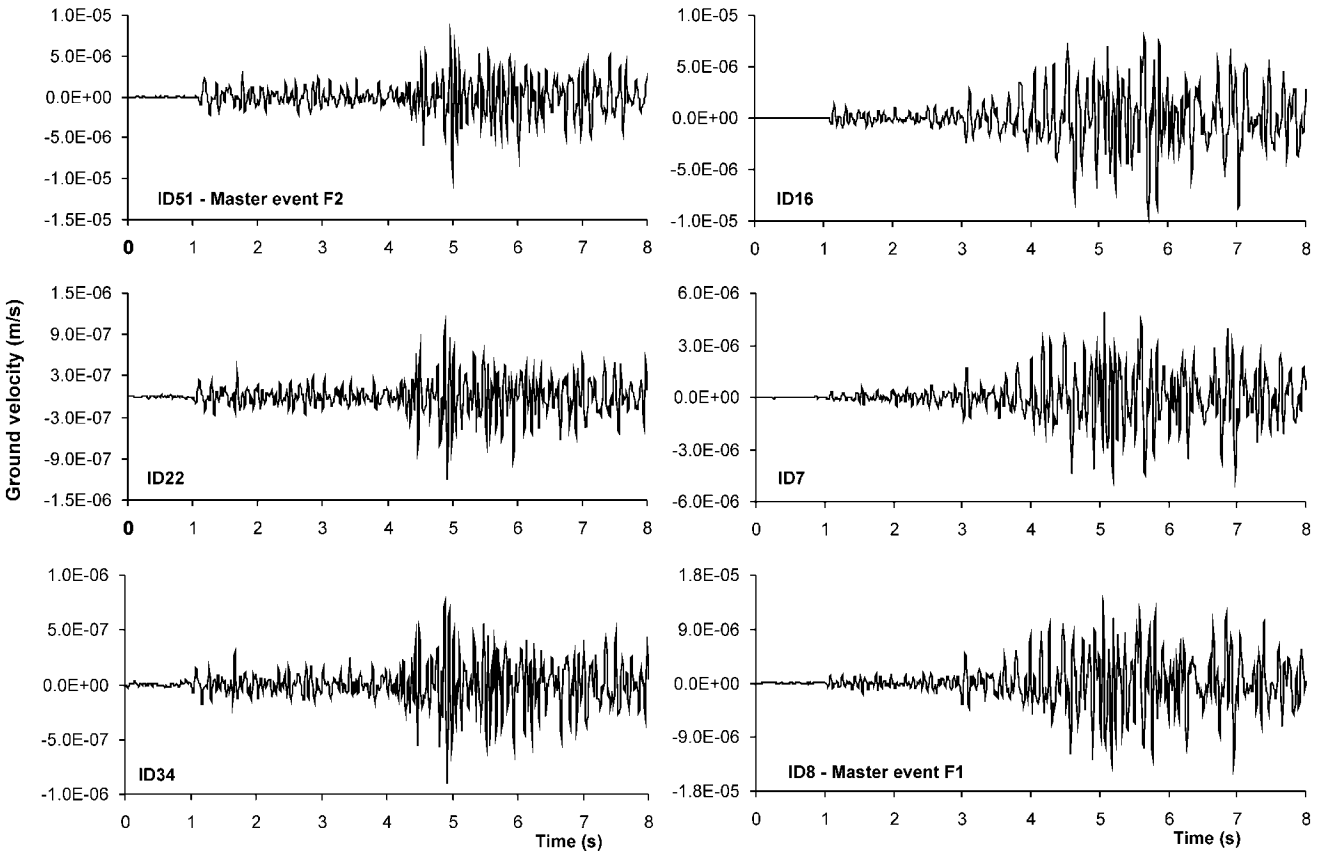

Figure 5. Comparison of events recorded at station SR2 (vertical component): (left) three earthquakes of the first swarm; (right) events of the second one. Note the high similarity of waveforms of events belonging to the same swarm.

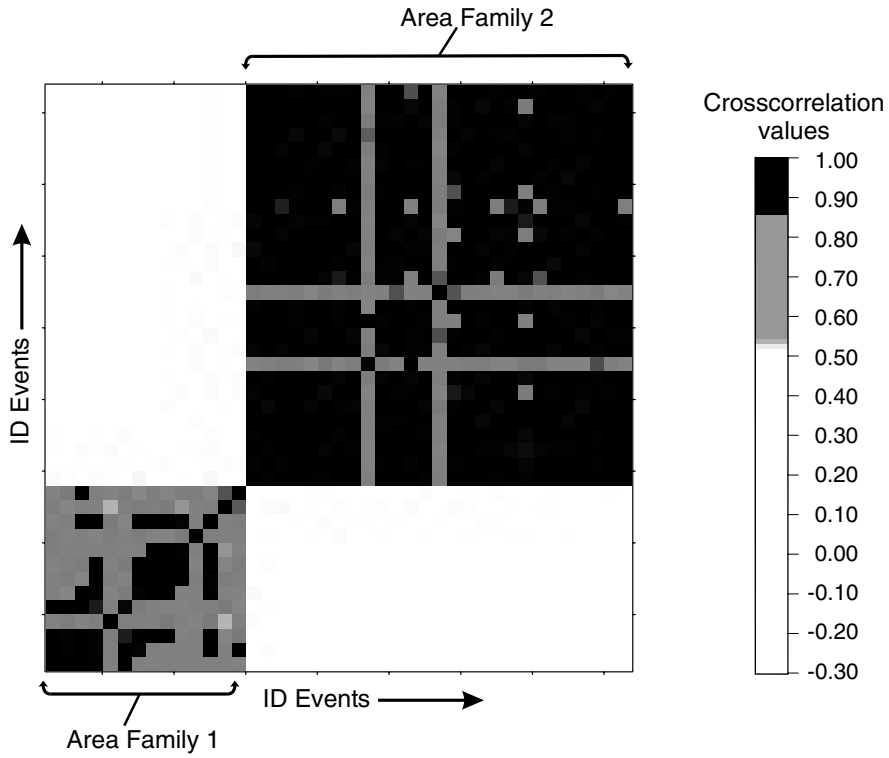

Figure 6. Graphical visualization of the correlation matrix obtained for station SR1.

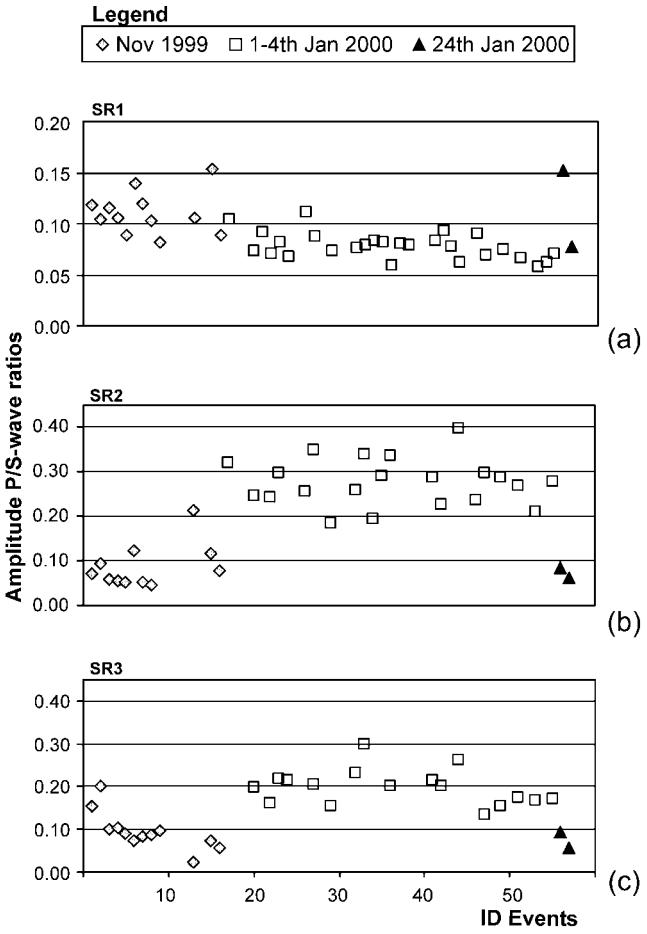

Figure 7. Plot of *P*/*S*-wave amplitude ratios at three key stations: (a) SR1, (b) SR2, and (c) SR3. Diamonds, squares, and triangles indicate the different periods of earthquake occurrence. The vertical scale for SR1 is doubled. Note the different trends for the events of November and January.

The refined calculation of time differences *dt* between master and slave events was performed following a method in two steps as proposed by Frémont and Malone (1987). After defining the window to be used., for example, the part with the first *P*-wave arrivals, a coarse phase alignment of the two traces is carried out in the time domain, taking into account the time differences, where the maximum correlation coefficient is obtained. In the second step we calculated the cross spectra and corrected the time differences from the slope of the phase of the cross spectra (see Frémont and Malone, 1987).

First attempts at relative locations using *P*-wave onsets failed, in particular for the lowest magnitude earthquakes, as the *P* onsets were emergent at various stations (i.e., SR4, SR5, SR6) and the signal-to-noise ratios were low. This inhibited a suitable phase alignment and made the cross-spectral analysis unstable. *S*-waves, on the other hand, generally offered considerably better signal-to-noise ratios and showed well-developed peaks (Fig. 9). With the cross-correlation technique, which is sensitive to the maximum or the centroid of the signal rather than to their first break, we can use *S*-wave arrivals even though their true onsets may be blurred by the *P*-wave coda or by *P*- to *S*-wave conversions. The estimated arrival times can be used with an accuracy comparable to the *P*-wave arrivals, as long as the arrival times are picked at exactly the same phase (which is the centroid of the *S*-wave train) in all seismograms recorded at a given station. Indeed the purpose of the cross correlation is to ensure that arrivals are determined identically for all events (Deichmann and Garcia-Fernandez, 1992).

We rotated the horizontal components, decomposing the signal into the longitudinal and transverse components and considered the latter, which is assumed to consist of only *SH* waves. Thus we avoid (or limit) the influence of possible disturbances that may arise from *P*-*SV* conversions. We selected event 8 (*M* 2.0) as master for family 1 and event 51 (*M* 2.0) as master event for family 2. The selection of the master events was based on the signal-to-noise ratio and, at the same time, the presence of as many as possible high correlation coefficients with the other events within the family. The time differences *dt* between the master and slave events were obtained using a signal window of 256 points (2.04 sec), corresponding to about 20 times the dominant period of the *S* wave, which was ~0.1 sec. The stability of the *dt* estimate is improved by shifting the window four times by an amount of 0.08 sec within the *S*-wave train and taking the average of the values of *dt* obtained for each window.

A measure of similarity between master and slave events is given by the quality of comparison *Q*, which is derived from the coherency $C(f)$, averaging the expression

$$C(f)^2/(1 - C(f)^2)$$

over the frequency band of interest (here between 1 and 20 Hz). In Figure 10 we show an example of two aligned doublet events. On the whole we got *Q* values between 90 and 100, corresponding to a coherency close to 1 over wide frequency bands.

Relative location of the two families was carried out on the basis of time differences obtained for the *SH* waves. The four unknown quantities (relative positions and difference in origin times) were determined using a singular value decomposition (for are explanation of the method, see Aki and Richards [1980] or Fréchet [1985]). The parameters used in the relocation technique are (1) takeoff angles and azimuths of stations from the reference event computed by a traditional location, (2) the wave velocity, and (3) the time differences *dt*. We obtain takeoff angles of more than 90° with respect to the negative vertical at all stations. In all relative locations we used an *S*-wave velocity of 3.6 km/sec around the hypocenter clusters. This is the corresponding V_S value in the velocity model by Musumeci *et al.* (2003). The choice of this value affects the size of the cluster linearly; for instance, with an *S*-wave velocity 10% higher the cluster di-

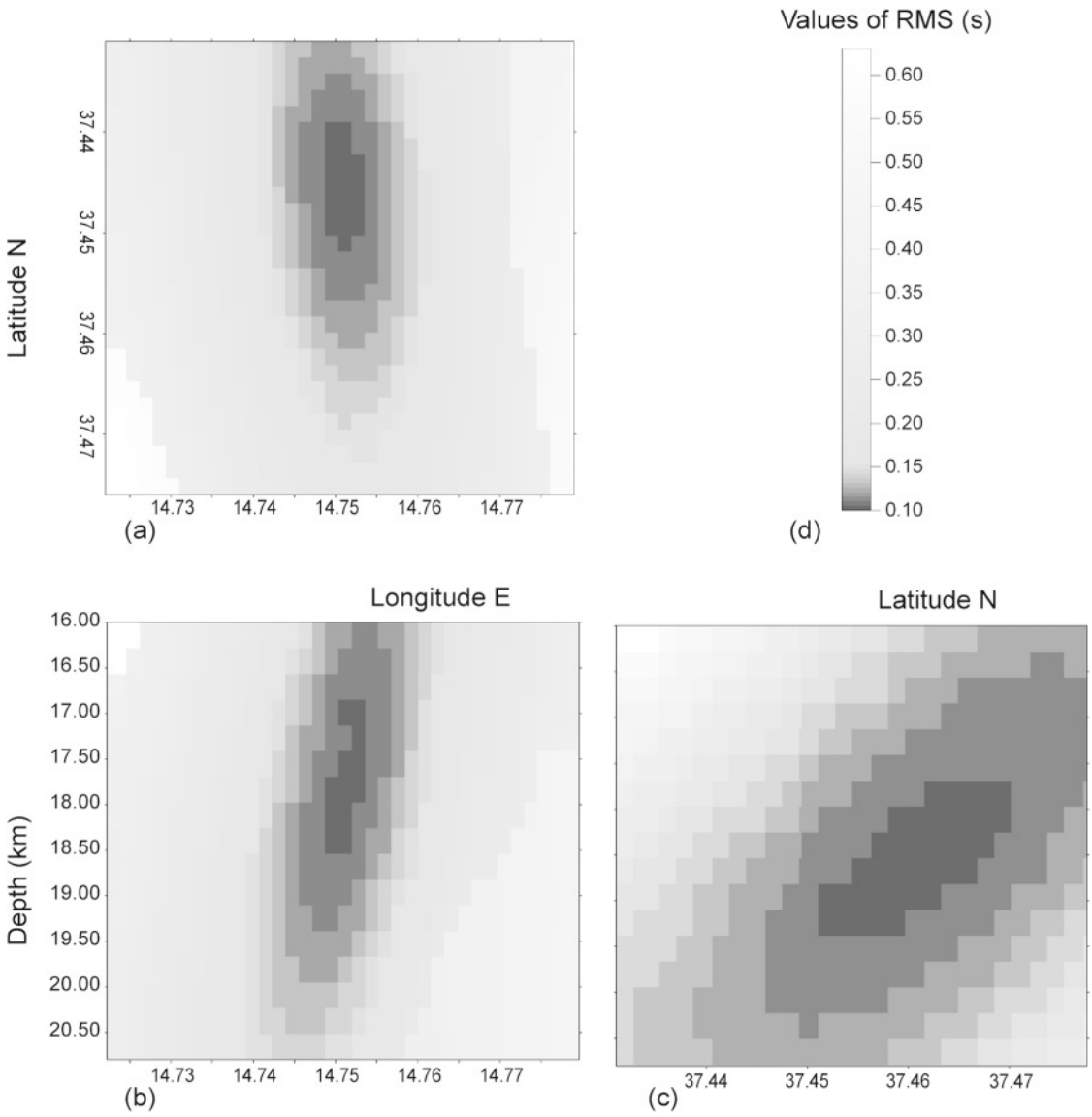

Figure 8. Plot of three cross sections of the residual cube obtained for event 1. The cross sections are oriented parallel to the Earth's surface (a) at 18.50 km of depth, vertically (b) in East–West and (c) North–South direction; darker shades indicate lower values of the residual, as reported (d) in the scale.

mensions increase 10% as well. The shape of the cluster and its orientation remain unaltered, however.

The relative relocations of the events in family 1 (swarm of November 1999 plus the events on 24 January 2000) are represented in an epicenter map and in two vertical cross sections (Fig. 11). Sixteen events out of 17 could be relocated relative to master event 8. The covariance matrix of the relative hypocenter locations is a way to represent the orientation of the "hypocenter cloud." In Table 2 the covariance matrices of the two clusters are represented in terms of their respective eigenvalues and eigenvectors. They provide a rough idea about the shape and orientation of the clusters. From both the plots one finds the 17 events arranged along a north-northwest–south-southeast–trending subvertical volume with a vertical extent of about 500 m and horizontal dimensions of about 200 and 80 m. From the relations between the largest and smallest eigenvalues (Table 2, top) we deduce that the hypocenters form a fairly well defined, slablike, planar element, whose thickness is less than 1/10 of its largest dimension. The eigenvectors reflect an orientation of the hypocenters similar to the distribution visible in the plots (Fig. 11). If we consider the plane spanned by the eigenvectors of λ_1 and λ_2, whose normal vector corresponds to the eigenvector of λ_3, we calculate a strike direction of the hypocenter cluster of N17°W and a dip of 84° E.

Family 2 consists of 27 events. Twelve remaining earthquakes had insufficient data for the relocation. The relation

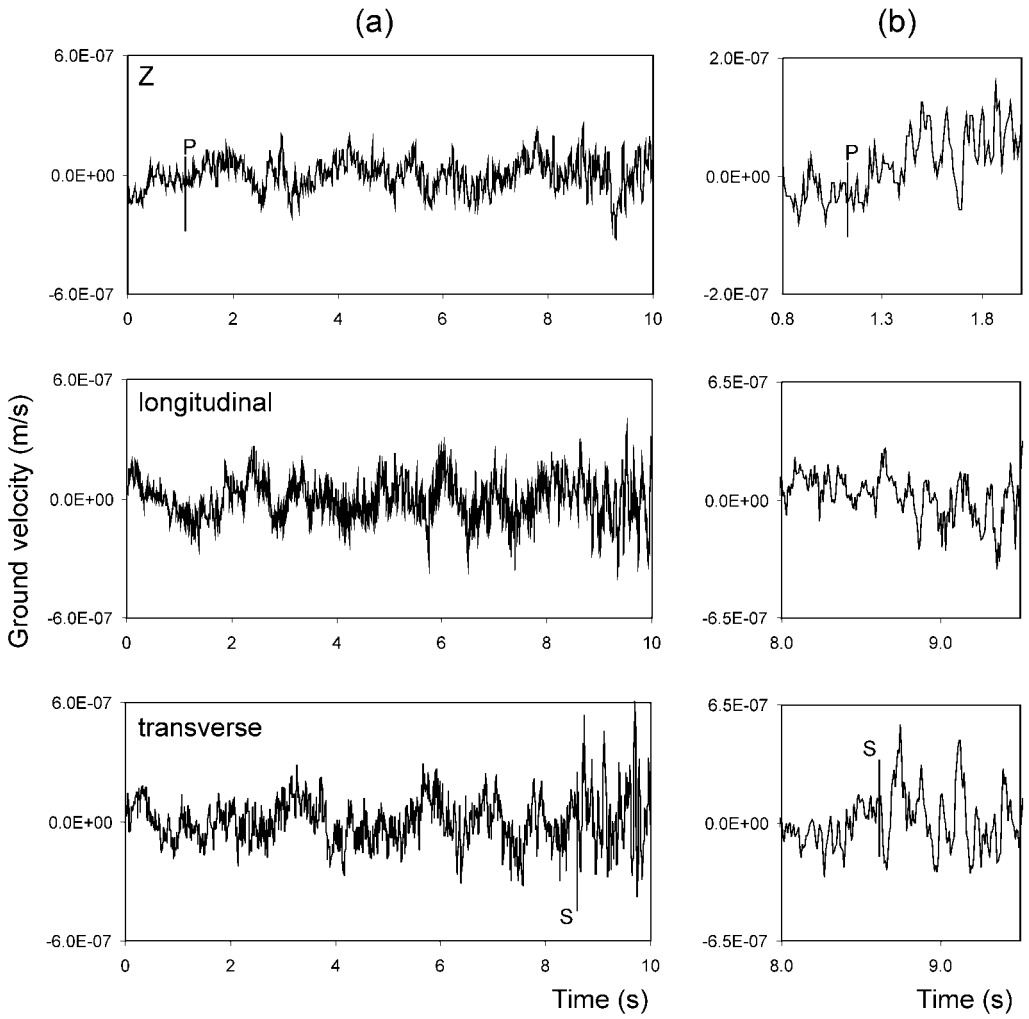

Figure 9. Example of a three-component record at station SR5: (a) 10 sec signal; (b) zooms of *P* and *S* first arrivals. Note the low signal-to-noise ratio for the *P* wave.

of the largest to the smallest eigenvalue (Table 2, bottom) indicates that the second cluster of hypocenters forms a more stocky body, with a lateral extent about 30% of its largest dimension. From the east-northeast–west-southwest section, however, one may identify, among the diffuse hypocenter cloud, a fairly tight linear element, whose orientation resembles the plane defined by family 1. Considering again the plane spanned by the eigenvectors of λ_1 and λ_2, and with the eigenvector of λ_3 as the normal vector, we obtain a strike direction of N19°W and a dip angle of 80° E. From the eigenvalues we derive dimensions of about 300 m in the northwest and about 250 m in the vertical direction (Fig. 12). The strong clustering of the foci is well evidenced in Figure 13, where the comparison with results from absolute location is shown.

As stated earlier, a more precise velocity model (Musumeci *et al.*, 2003) was used here to relocate the events. The computed azimuth and incidence angles of the first *P* phases underwent changes at several stations with respect to Scarfì *et al.* (2001). We computed two composite fault-plane solutions by combining the *P*-onset polarities of the two families defined on the basis of waveform analysis and *P*/*S*-wave amplitude ratios. The fault-plane solutions were obtained using the program FPFIT by Reasenberg and Oppenheimer (1985); they are shown in Figure 14a. The events of family 1 reveal a mechanism that can be interpreted as right-lateral slip along a north-northwest–south-southeast–trending plane. On the other hand, the earthquakes of family 2 show a normal faulting mechanism, also in this case along a north-northwest–south-southeast–trending plane. A few polarities in the composite solutions contradict the general behavior of the families; these divergent polarity readings are due to their poor quality because of the emergent onset of first *P*-wave arrivals and the low signal-to-noise ratio. Given the limited number of polarities and the azimuthal gap, one can argue that the reliability of the fault-plane solutions is low. In Figure 14b we show the composite fault-plane solutions that were obtained using the coordinates of the master events plus the relative offsets of the slave events. Although we did not reinterpret the polarities (in the sense

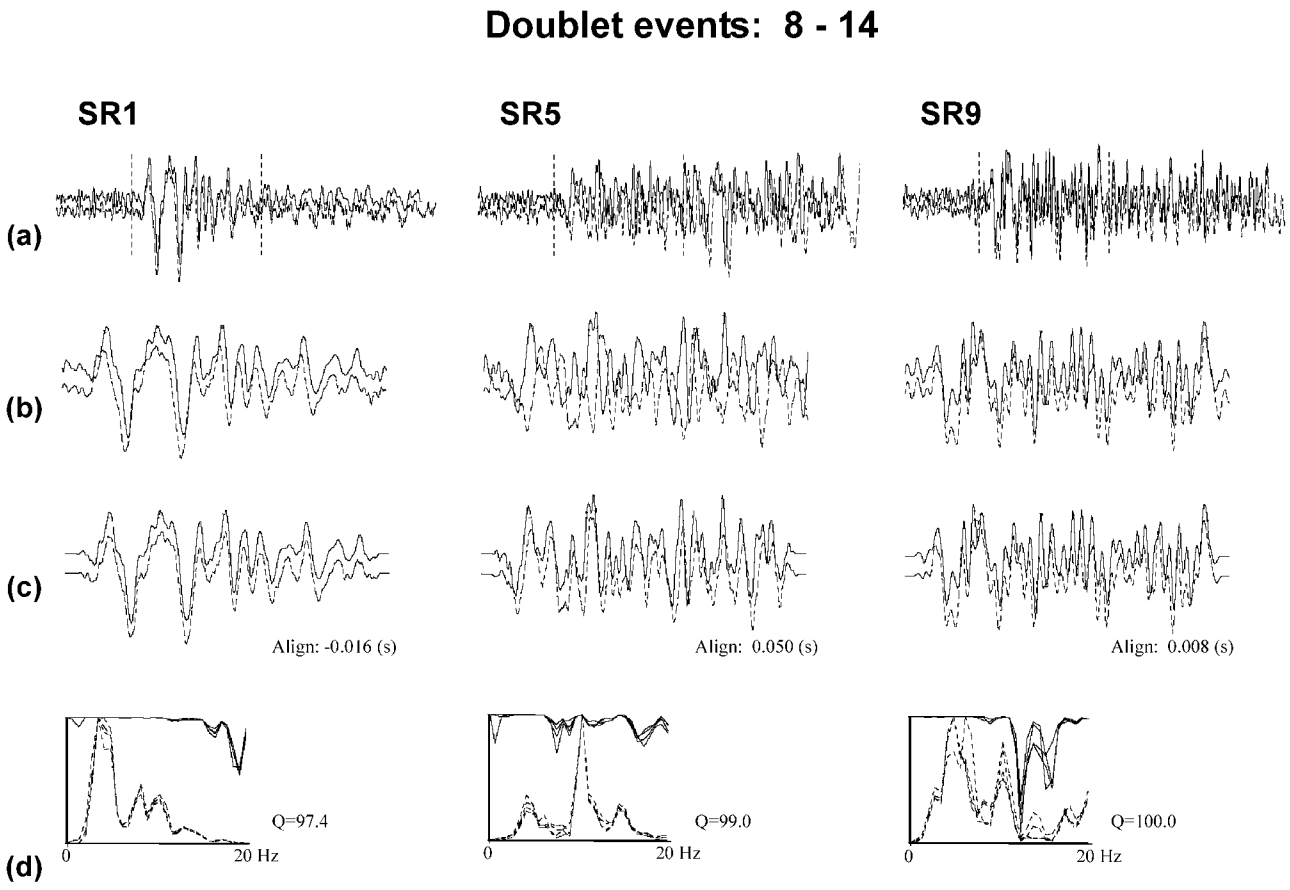

Figure 10. Examples of high-precision time picking at three stations (SR1, SR5, SR9), with event 8 as master and event 14 as slave event. (a) Overall view of the *S* phases at the three stations, (b) zoomed-in image of initial alignments, (c) zoomed-in image of realignments, (d) the four cross spectra (dotted lines) and coherency spectra (solid lines) obtained for the four shifted windows (see text). Note the almost flat coherency spectra in the frequency range between 0 and 15 Hz. *Q* values are understood as averages over the four windows.

of unifying polarities of events belonging to the same family), the scatter of the data points in the stereographic projections is reduced. This is to be expected, as the differences between events belonging to a family almost vanish. We further note that the composite solutions of the two families turn out to be more similar than the two solutions in Figure 14a. Indeed, the two similar fault-plane solutions that we obtained may represent further evidence of a common mechanism responsible for the two distinct earthquake clusters.

Analysis of Location Uncertainties

The accuracy of time picking may depend on various factors, such as limits of the time resolution of the clocks and drift or variations in instrumental characteristics. The time resolution of the clocks is reported by the manufacturer of the data acquisition equipment to be as precise as 1 msec, and the drift should be of minor importance, as the time difference among the events within the clusters is largely less than 1–2 days. The network characteristics remained constant, as there was no replacement of instruments during the time of interest. Other variations, for example, caused by seasonal effects (temperature changes between winter and summer), can be neglected, as both swarms occurred in the colder season from November to January. However, the shape of the hypocenter clusters resembles to some extent the orientation of the rms minimum obtained carrying out the grid search location earlier. One may suspect that some uncertainties of time picking may have escaped the attention of the operators, and the hypocenter cluster geometries may be an artifact of the station configuration.

The relative location succeeded with small residuals, typically no more than 1–2 m, for almost all slave events of both families. Given the somewhat unfavorable distribution of SESSN stations with respect to the two studied swarms, one may suspect that the computed extension of the clusters (and the related uncertainty) are partly an artifact of a non-optimally constrained inversion. Therefore we have tested the stability of our relocation by performing a Monte Carlo experiment in which we conducted three random tests,

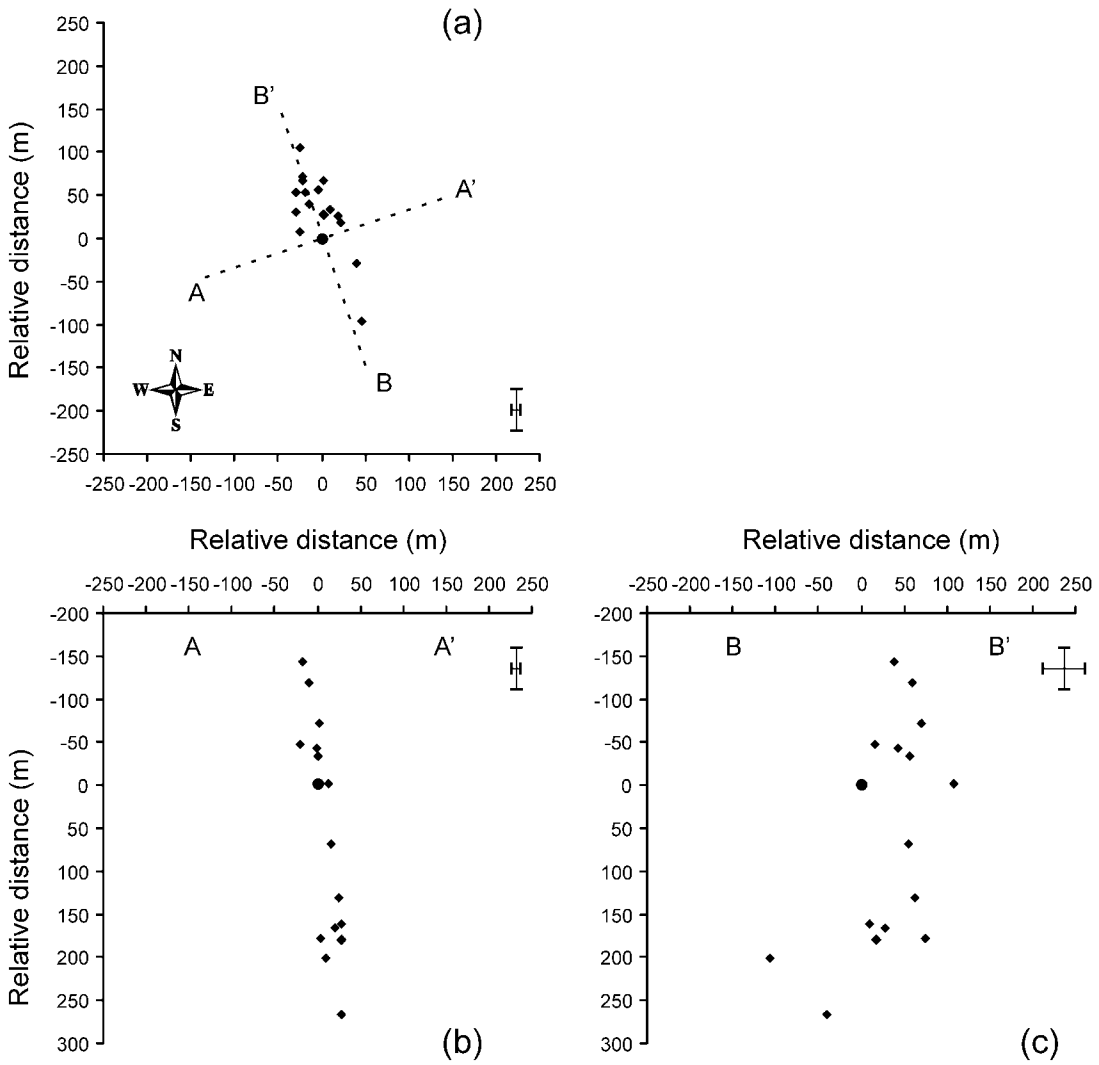

Figure 11. Relative locations of family 1 using the cross-spectral technique without adding random perturbations to time pickings; (a) map view and (b, c) vertical cross sections. The master event is indicated with a solid circle. The error bars represent the uncertainties of the relative locations as inferred from the Montecarlo experiment with an inaccuracy of time picking of up to 5 ms (see also Table 3).

choosing three events with the lowest, intermediate, and highest residuals, respectively. We repeated relative relocations, adding random uncertainties to the originally obtained travel-time differences *dt* in the ranges of ± 100, 20, and 5 msec. The statistics of our Monte Carlo experiment are summarized in Table 3. In all cases the *Y* (latitude) and *Z* (vertical) components exhibit the greatest instability, whereas the *X* (longitude) shows only minor scatter. This is again not surprising, considering the somewhat unfavorable station configuration with respect to the Ramacca swarms. The relocation experiments where the inaccuracy of phase differences was assumed to be up to 100 and 20 msec, yield significantly higher residuals (i.e., 18–26 and 3.4–6 m, respectively) than the original relocation without random perturbation (residual less than 2 m). When an inaccuracy of time picking in the range of ± 5 msec is assumed, the residuals remain on the same order of original ones, that is, 1–2 m. In this case the solutions scatter with a standard deviation of about 50 m in the *Y* and *Z* directions, which is on the order of the second eigenvalue of family 1, but significantly less than the dimensions of family 2 as inferred from its three eigenvalues. The scatter of less than 10 m in the *X* direction is of the same order as the lateral extent of family 1 but by far less than that of family 2.

In a further step of the experiment we repeated the relocation, changing the master events in both families. In particular, we replaced master event 8 (Table 4) with event 3 in family 1 and event 51 with event 27 in family 2. In Table 4 we report the relative changes of relative coordinates for both families, expressed with respect to the original master

Table 2
Eigenvalues, Dimensions, and Eigenvectors

λ(m^2)	$2\sqrt{\lambda}$ (m)	e^T		
Family 1*				
21239	288	0.1344	−0.1404	0.9809
1897	87	−0.2575	0.9509	0.1714
99	20	−0.9569	−0.2757	0.0917
Family 2†				
6487	161	0.2159	−0.8623	−0.4580
1878	86	0.2892	−0.3916	0.8735
564	47	−0.9326	−0.3210	0.1649

The three components of the eigenvectors are the direction cosines measured to three axis x_1 (east–west), x_2 (north–south), and x_3 (vertical).
*Corresponding strike and dip of planar element: N17°W; 84° E
†Corresponding strike and dip of planar element: N19°W; 80° E

events. Except for two single events, the differences of the relocations are of the same order as the scatter of solutions found in the Monte Carlo experiment using an assumed time inaccuracy of 5 msec. In other words, the dimensions of family 2 in the vertical and north–south direction are significantly larger than the uncertainties inferred by comparing relocations using two different master events. The same holds for the vertical extent of family 1 of about 500 m, whereas its horizontal extents are rather narrow.

Discussion and Conclusions

Southeastern Sicily has been struck several times by devastating earthquakes (M up to 7.5) in the past millennium. Accurate interpretation of seismicity patterns in this

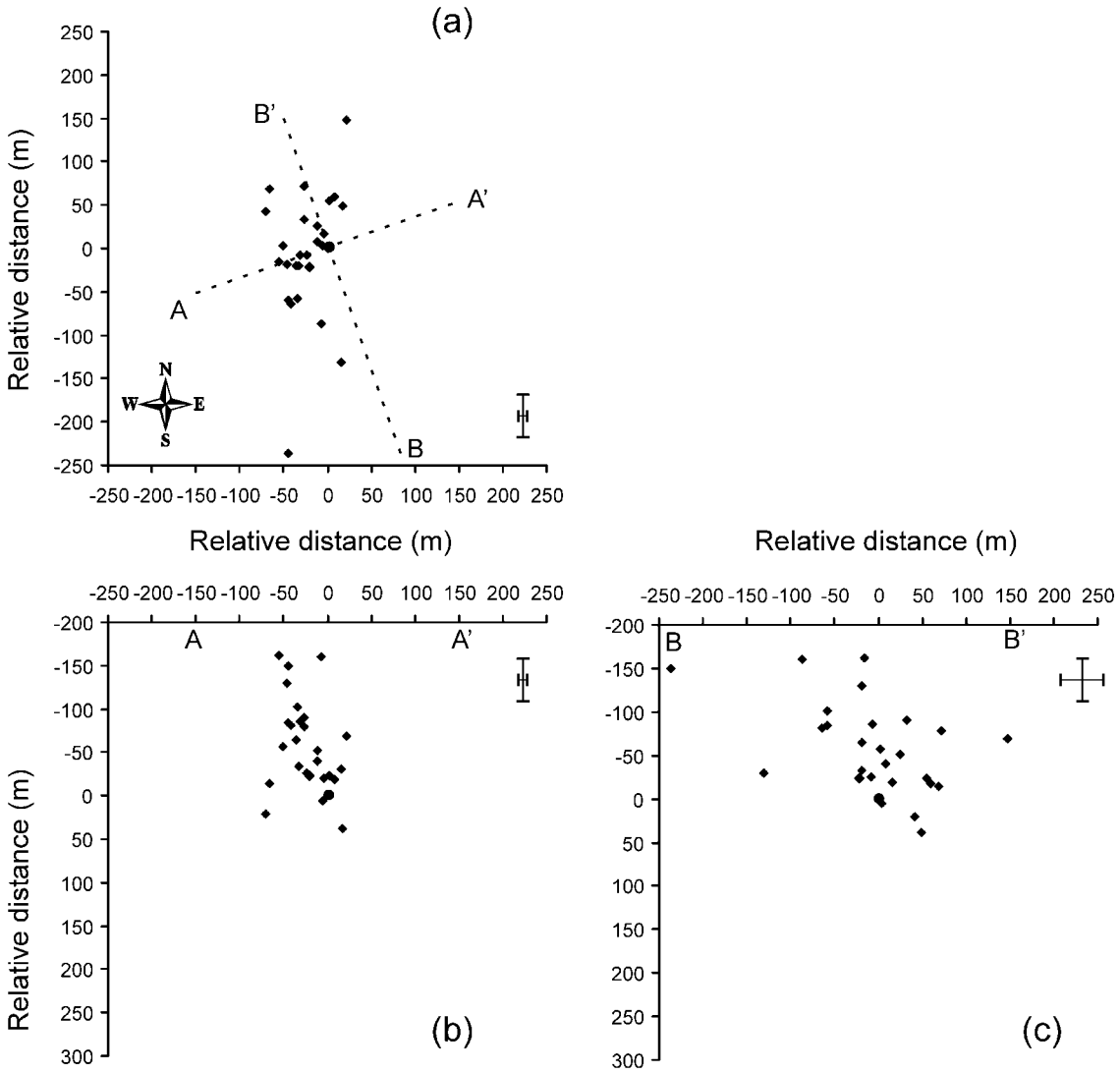

Figure 12. The same as in Figure 11, but for family 2.

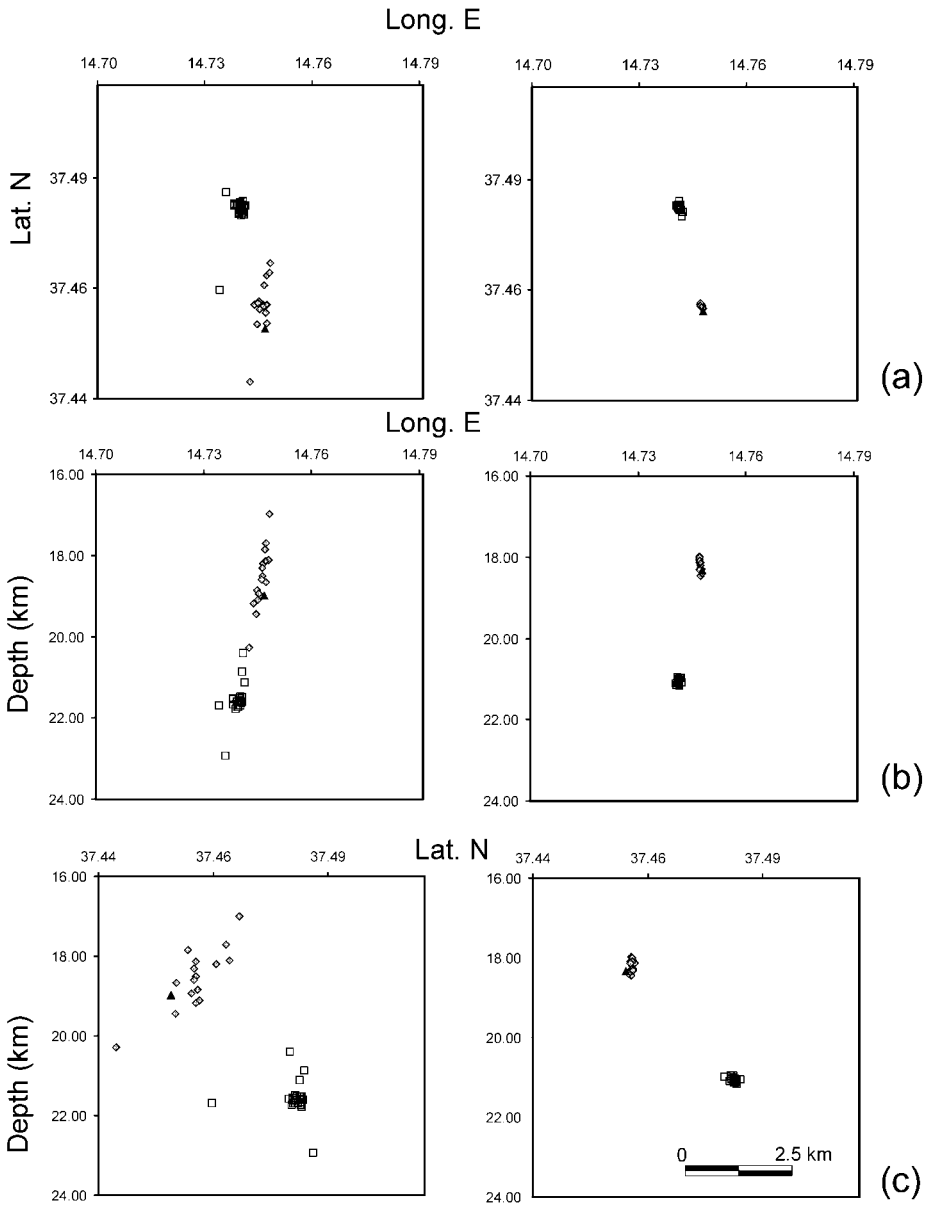

Figure 13. Comparison of absolute (left) and relative (right) locations for the two earthquake families; (a) epicenter map, (b) West–East and (c) South–North vertical cross sections. The symbols are the same as in Figure 4.

region is therefore important for assessing the potential for large earthquakes. The main purpose of this work has been to reconstruct the source geometry of two seismic swarms that occurred in November 1999 and January 2000 at the site of Ramacca.

From standard location techniques, the two swarms form two north–south elongated hypocenter clusters centered at depth of about 19 and 22 km, respectively. At first glance, one could interpret the north–south alignment as a hypothetical northern continuation of the Scicli regional fault system, buried under the thrust nappes of the northern mountain chain. It can be shown, however, that the apparent shape of the two hypocenter clusters is probably an artifact of the nonideal station configuration of the network with respect to the location of the swarms. From the analysis of many very similar waveforms we conclude that most events of the swarms are multiplet events, clustered closely together, with similar extensional focal mechanisms. The first family included 16 events and occurred in November 1999 plus two on 24 January 2000. The other family occurred at the beginning of January 2000.

As standard location procedures fail to resolve the geometry of closely spaced earthquakes, we have performed high-precision relative locations following the method by

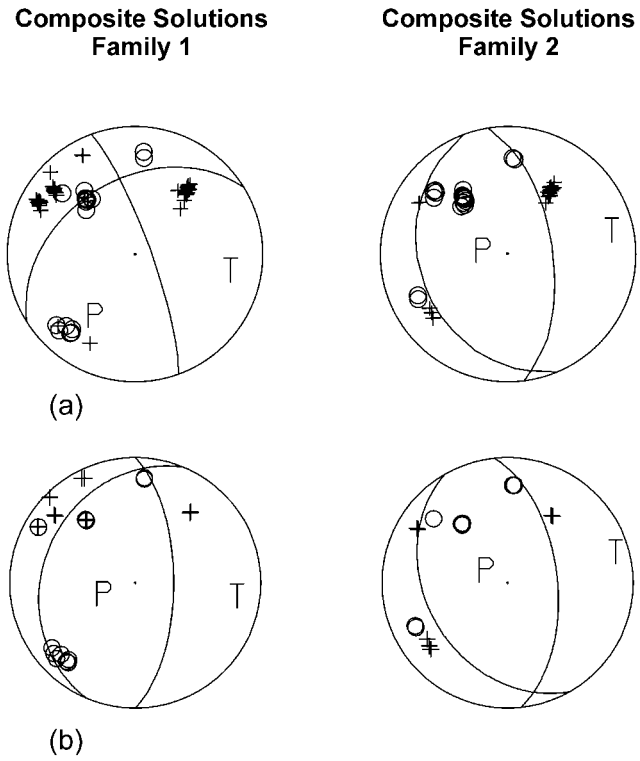

Figure 14. Composite fault-plane solution mechanism (lower hemisphere projection) of the two earthquakes families (+ for compression, O for dilatation). (a) using absolute locations, (b) using relative locations.

Table 4
Variations in Relative Coordinates for Both Families Obtained by Changing the Master Events

Family 1				Family 2			
ID	*X* (m)	*Y* (m)	*Z* (m)	ID	*X* (m)	*Y* (m)	*Z* (m)
1	−7.6	31.96	−20.05	18	4.16	−18.19	−3.84
2	−5.18	16.14	−17.84	19	5.53	−8.75	−11.7
3	0	0	0	20	1.4	6.6	10.22
4	1.1	−12.53	−3.43	22	4.05	−14.72	−5.45
5	−8.21	75.69	−27.97	23	−3.2	3.68	15.49
6	−2.57	−17.35	−3.36	24	1.24	4.4	2.98
7	−1.94	−5.16	3.94	25	−0.41	−1.07	4.62
8	−2	4.44	−0.99	26	5.69	−20.37	−7.83
9	−4.01	6.68	2.82	27	0	0	0
10	−8.7	5.55	6.5	28	11.56	−123.14	−57.89
11	−6.68	50.07	−4.02	29	−11.75	8.82	32.01
12	−11.66	25.08	9.83	30	−0.94	10.23	10.3
13	−12.01	−81.63	22.39	31	−0.39	−9.51	2.89
14	−10.76	2.9	15.91	32	−2.99	14.07	30.03
16	−13.47	45.67	−25.73	34	1.23	−2.84	22.83
				36	−3.22	−11.59	4.98
				39	2.98	−7.36	−6.72
				40	−1.47	−3.72	5.31
				41	−2.98	2.44	15.54
				47	2.07	−12.94	7.19
				48	3.91	−6.96	0.87
				49	0.64	−4.66	10.43
				50	−4.04	−4.19	15.98
				51	1.8	−4.06	−0.76
				52	−2.69	−1.41	−1.29
				53	−5.38	−9.54	17.34
				55	−0.91	8.36	2.19

Table 3
Statistics of the Monte Carlo Experiment

	σ_X (m)	σ_Y (m)	σ_Z (m)	Res. (m)
		$dt \pm$ max 100 msec		
Event 3	124.98	667.46	696.96	26.04
Event 7	129.83	443.88	620.38	18.27
Event 13	113.79	565.86	457.04	24.62
		$dt \pm$ max 20 msec		
Event 3	25.48	135.51	140.62	6.00
Event 7	24.81	99.09	118.65	3.46
Event 13	21.53	127.58	86.84	6.00
		$dt \pm$ max 5 msec		
Event 3	6.02	34.10	34.69	2.17
Event 7	7.14	22.94	32.03	1.15
Event 13	7.15	68.13	27.93	2.29

The standard deviation is in the *X, Y*, and *Z* axes and in residuals of the relative locations (see text for further explanations).

Frémont and Malone (1987). For reasons of signal quality we have used *SH* waves rather than *P* waves, obtaining excellent degrees of coherence, typically above 0.95 over wide frequency ranges. Typically six stations could be used for the relocations, obtaining residuals of 1 m (on average) and no more than 2 m in the worst case. From the relocation we obtained two tight clusters. We express their spatial dimensions in terms of the eigenvalues and eigenvectors of the covariance matrices calculated from the coordinates relative to the master event. The first cluster corresponds to a vertically oriented planar volume with a vertical extent of about 500 m and horizontal dimensions of about 200 m and 80 m. The second cluster forms a more stocky body with dimensions of about 300 m and 120 m in the north-northwest–south-southeast and east-northeast–west-southwest directions, respectively, and about 250 m in the vertical direction.

Despite the fairly low residuals, we must be aware of possible biases introduced by the station configuration and inaccuracy of time reading. In order to simulate the presence of possible errors, we have carried out a series of Monte Carlo experiments, adding a random number to time differences originally used in the relocation. From a comparison of the original relocation residuals with those using perturbed time differences, we concluded that the inaccuracy (if any) is not larger than ± 5 msec. Admitting such a random perturbation, we get an actual inaccuracy of about ± 10 m in longitude and about ± 50 m in latitude and depth, which is about twenty to fifty times less than the formal absolute location error. Similar results are obtained if we compare relocations carried out with different master events. In the end, we conclude that the inaccuracy of time differ-

ences should not exceed the range of ± 5 msec; therefore, the extents of the seismogenic source regions beyond the estimated uncertainties are not artifacts, but reflect the true geometries of the families. In particular we find the vertical extents of both families to be robust, as is the north–south elongation of family 2. The shapes and orientations are thus in agreement with trends inferred from the focal mechanisms.

From the relative relocations we may trace the temporal migration of hypocenters of the two families (Fig. 15). In family 1 we note a clear shoaling of hypocenters (about 320 m in 14 hr) as the swarm progresses. Family 2 shows a slightly more complex trend: an upward migration of foci for the first 14 events only (about 110 m in 2 hr); then further activation of the lower parts of the cluster extending through the whole rupture volume (Fig. 15). The migration in the vertical direction can be related to the characteristics of normal faulting inferred from the composite fault-plane solutions. On the other hand, no substantial horizontal migration of the foci is observed.

The migration of hypocenters as observed here has been explained by Nishigami (1987), who proposed a cluster source model with patches representing the areas on the fault plane having relatively high strength. These asperities are

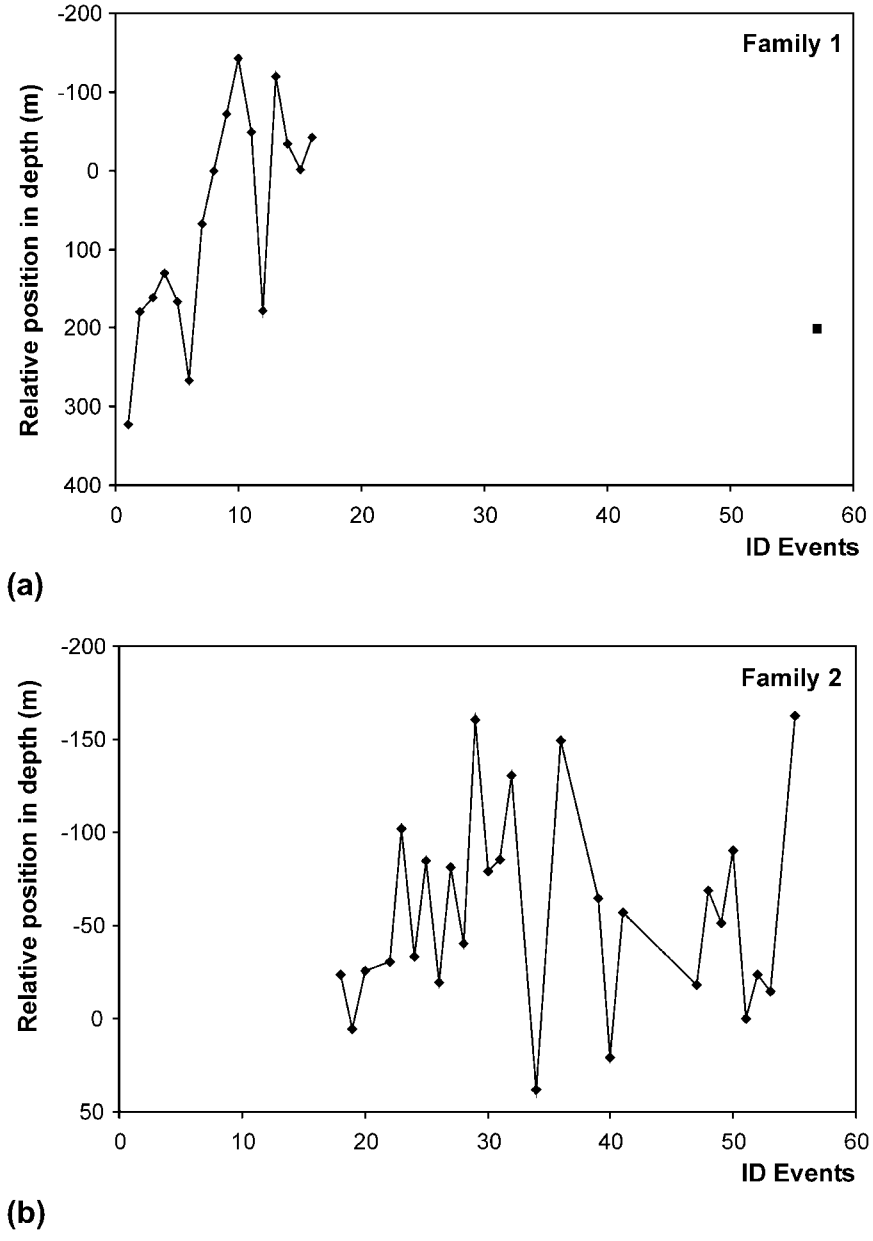

Figure 15. Time sequence of the relative depth with respect to the master events for (a) family 1 and (b) family 2. Note the different vertical scales. For the absolute time of the events, refer to Table 1.

expected to resist the complete sliding of the fault plane and are to become the initiation points of subsequent ruptures owing to the stress concentration. On the other hand, swarms are often seen as a consequence of an increase of pore pressure caused by fluid flow (e.g., Hill, 1977). As the strain release is controlled by the fluid flow, no dominant earthquake may develop (see Scholz, 1990).

The hypothesis that the Ramacca swarms are related to fluid flow may be supported by the intense basaltic volcanic activity during the Late Cretaceous, upper Miocene, and Pliocene that characterized (Fig. 1) the Hyblean Plateau (Scribano, 1987; Grasso *et al.*, 1990). A residual of this activity is the geothermal fields of Mineo (Pedley and Grasso, 1991), situated about 10 km south of the epicenters of the Ramacca swarms (Fig. 2). These fields are characterized by a low-enthalpy geothermal anomaly, with significant carbon dioxide sources. Moreover, geochemical surveys performed after the 13 December 1990 local earthquake evidenced the activation of fluid flow of deep origin, which moved upward along regional structural tectonic elements (Dall'Aglio *et al.*, 1995).

Considering the focal depth (from 17 to 22 km) of the clusters and the upward foci migration of the events, we propose that movement of fluids of plutonic origin may have provided the triggering mechanism for these swarms. The distribution of fluid overpressures in the crust exerts a strong influence in the style of faulting, and normal faults have been shown to be easily activated by volumetric mesh structures (Sibson, 1996).

Acknowledgments

We wish to thank Dr. Stephanie G. Prejean and an anonymous reviewer for their constructive criticism. Helpful suggestions by Dr. Charlotte Rowe are greatly appreciated, too. Francesca Ghisetti and Rick Sibson are kindly acknowledged for fruitful discussion and the accurate revision of the English text. We also wish to thank Steve Malone, who provided us with the software of the cross-spectrum technique and gave important hints concerning the use and possible pitfalls of the method. S.G. was financially supported by Catania University grants (fondi di Ateneo 2001).

References

Aki, K., and P. G. Richards (1980). *Quantitative Seismology: Theory and Methods*, W. H. Freeman, New York, 932 pp.

Amato, A., R. Azzara, A. Basili, C. Chiarabba, M. Cocco, M. Di Bona, and G. Selvaggi (1995). Main shock and aftershocks of the December 13, 1990, Eastern Sicily earthquake, *Ann. Geofis.* **38,** 255–266.

Azzaro, R., and M. S. Barbano (2000). Analysis of the seismicity of southeastern Sicily: a proposed tectonic interpretation, *Ann. Geofis.* **43,** 171–188.

Barbano, M. S., and R. Rigano (2001). Earthquake sources and seismic hazard in southeastern Sicily, *Ann. Geofis.* **44,** 723–738.

Ben-Avraham, Z., V. Lyakhovsky, and M. Grasso (1995). Simulation of collision zone segmentation in the central Mediterranean, *Tectonophysics* **243,** 57–68.

Bianca, M., C. Monaco, L. Tortorici, and L. Cernobori (1999). Quaternary normal faulting in southeastern Sicily (Italy): a seismic source for the 1693 large earthquake, *Geophys. J. Int.* **139,** 370–394.

Cogan, J., L. Rigo, M. Grasso, and I. Lerche (1989). Flexural tectonics of southeastern Sicily, *J. Geodyn.* **11,** 189–241.

Console, R., and R. Di Giovambattista (1987). Local earthquake relative location by digital records, *Phys.Earth Planet. Inter.* **47,** 43–49.

Dall'Aglio, M., F. Quattrocchi, and S. Tersigni (1995). Geochemical evolution of groundwater of the Iblean Foreland (Southeastern Sicily) after the December 13, 1990 earthquake ($M = 5.4$), *Ann. Geofis.* **28,** 309–329.

Deichmann, N., and M. Garcia-Fernandez (1992). Rupture geometry from high-precision relative hypocentre locations of microearthquake rupture, *Geophys. J. Int.* **110,** 501–517.

Fréchet, J. (1985). Sismogenese et doublets sismiques, *Ph.D. Thesis*, University of Grenoble.

Frémont, M. J. (1984). Mesure de variations temporelles des paramètres de la croute terrestre et d'effects de sources par traitement de doublets de sèismes, *Ph.D. Thesis*, University of Grenoble.

Frémont, M. J., and S. D. Malone (1987). High precision relative locations of earthquakes at Mount St. Helens, Washington, *J. Geophys. Res.* **92,** 10,223–10,236.

Geller, R. J., and C. S. Mueller (1980). Four similar earthquakes in Central California, *Geophys. Res. Lett.* **7,** 821–824.

Ghisetti, F., and L. Vezzani (1980). The structural features of the Iblean plateau and of the Monte Iudica area (South Eastern Sicily). a microtectonic contribution to the deformational history of the Calabrian Arc, *Boll. Soc. Geol. It.* **99,** 57–102.

Got, J. L., M. Fréchet, and F. W. Klein (1994). Deep fault plane geometry inferred from multiplet relative relocation beneath the south flank of Kilauea, *J. Geophys. Res.* **99,** 15,375–15,386.

Got, J. L., P. Okubo, R. Machenbaum, and W. Tanigawa (2002). A real-time procedure for progressive multiplet relative relocation at the Hawaiian Volcano Observatory, *Bull. Seism. Soc. Am.* **92,** 2019–2026.

Grasso, M., and C. D. Reuther (1988). The western margin of Hyblean plateau: a neotectonic transform system on the SE Sicilian foreland, *Ann. Tectonicae* **2,** 107–120.

Grasso, M., A. De Dominicis, and G. Mazzoldi (1990). Structures and tectonic setting of the western margin of the Hyblean-Malta shelf, Central Mediterranean, *Ann. Tectonicae* **4,** 140–154.

Hill, D. P. (1977). A model for earthquake swarms, *J. Geophys. Res.* **82,** 1347–1352.

Hirn, A., R. Nicolich, J. Gallart, M. Laigle, L. Cernobori, and ETNASEIS Scientific Group (1997). Roots of Etna volcano in faults of great earthquakes, *Earth Planet. Sci. Lett.* **148,** 171–191.

Ito, A. (1985). High resolution relative hypocenters of similar earthquakes by cross-spectral analysis method, *J. Phys. Earth* **33,** 279–294.

Lentini, F., S. Carbone, and S. Catalano (1994). Main structural domains of the central mediterranean region and their tectonic evolution, *Boll. Geofis. Teor. Appl.* **36,** 103–125.

Musumeci, C., G. Di Grazia, and S. Gresta (2003). Minimum 1D velocity model in southeastern Sicily (Italy) from local earthquake data, *J. Seismol.* **7,** no. 3 (in press).

Nishigami, K. (1987). Clustering structure and fracture process of microearthquake sequences, *J. Phys. Earth* **35,** 425–448.

Pechmann, J. C., and H. Kanamori (1982). Waveforms and spectra of preshocks and aftershocks of the 1979 Imperial Valley, California, earthquake: evidence for fault heterogeneity? *J. Geophys. Res.* **87,** 10,579–10,597.

Pedley, M., and M. Grasso (1991). Sea-level change around the margins of the Catania–Gela trough and Hyblean Plateau, southeast Sicily (African–European plate convergence zone): a problem of Plio-Quaternary plate buoyancy? *Spec. Publ. Int. Ass. Sediment*. **12,** 451–464.

Phillips, W. S. (2000). Precise microearthquake location and fluid flow in the geothermal reservoir at Soultz-sous-Forêts, France, *Bull. Seism. Soc. Am.* **90**(1), 212–228.

Poupinet, G., W. L. Ellsworth, and J. Fréchet (1984). Monitoring velocity variations in the crust using earthquake doublets: an application to the Calaveras fault, California, *J. Geophys. Res.* **89,** 5719–5731.

Poupinet, G., J. Fréchet, W. L. Ellsworth, M. J. Frémont, and F. Glangeaud (1985). Doublet analysis: improved accuracy for earthquake prediction studies, *Earthquake Predict. Res.* **3,** 147–159.

Ragg, S., M. Grasso, and B. Müller (1999). Patterns of tectonic stress in Sicily from borehole breakout observations and finite element modeling, *Tectonics* **18,** 669–685.

Reasenberg, P. A., and D. Oppenheimer (1985). FPFIT, FPPLOT, and FPPAGE: Fortran computer progams for calculating and displaying earthquake fault-plane solutions, *U.S. Geol. Surv. Open-File Rept 85/379*, 109 pp.

Richter, C. F. (1958). *Elementary Seismology*, W. H. Freeman, New York, 768 pp.

Ross, S. L., A. J. Michael, W. L. Ellsworth, B. Julian, F. Klein, D. Oppenheimer, and K. Richards-Dinger (2001). Effects of initial location error and station distribution on double-difference earthquake relocations: comparing the San Gregorio and Calaveras Faults, *Seism. Res. Lett.* **72,** 291–292.

Rowe, C. A., R. C. Aster, W. S. Phillips, R. H. Jones, B. Borchers, and M. C. Felher (2002). Using automated high-precision repicking to improve delineation of microseismic structures at the Soultz geothermal reseirvoir, *Pure Appl. Geophys.* **159,** 517–541.

Scandone, P., E. Patacca, R. Radoicic, W. B. F. Ryan, M. B. Cita, M. Rawson, H. Chezar, E. Miller, J. McKenzie, and S. Rossi (1981). Mesozoic and Cenozoic rocks from Malta Escarpment (Central Mediterranean), *Am. Assoc. Petrol. Geol. Bull.* **65,** 1299–1319.

Scarfì, L., H. Langer, G. Di Grazia, A. Ursino, and S. Gresta (2001). Analysis of two microearthquake swarms in southeastern Sicily: evidence for active faults? *Ann. Geofis.* **44,** 671–686.

Scherbaum, F., and J. Wendler (1986). Cross-spectral analysis of Swabian Jura (SW Germany) three-component microearthquake recordings, *J. Geophys.* **60,** 157–166.

Scholz, C. H. (1990). *The Mechanics of Earthquakes and Faulting*, Cambridge U Press, New York, 439 pp.

Scribano, V. (1987). Ultramafic and mafic xenoliths in the alkaline volcanic rocks from the Hyblean Plateau (Sicily): a contribution to the knowledge of the upper mantle and deep crust, *Mem. Soc. Geol. It.* **38,** 475–482.

Sibson, R. H. (1996). Structural permeability of fluid-driven fault-fracture meshes, *J. Struct. Geol.* **18,** 1031–1042.

Sirovich, L., and F. Pettenati (1999). Seismotectonic outline of southeastern Sicily: an evaluation of available options for the earthquake fault rupture scenario, *J. Seismol.* **3,** 213–233.

Tsujiura, M. (1983a). Waveform and spectral features of earthquake swarms and foreshocks: in special reference to earthquake prediction, *Bull. Earth. Res. Inst. Tokyo Univ.* **58,** 65–133.

Tsujiura, M. (1983b). Characteristic frequencies for earthquake families and their tectonic implications: evidence from earthquake swarms in the Kanto District Japan, *Pure Appl. Geophys.* **4,** 573–600.

Waldhauser, F., and W. L. Ellsworth (2000). A double-difference earthquake location algorithm: method and application to North Hayward Fault, California, *Bull. Seism. Soc. Am.* **90,** 1353–1368

Yellin-Dror, A., M. Grasso, Z. Ben-Avraham, and G. Tibor (1997). The subsidence history of the northern Hyblean Plateau margin, eastern Sicily, *Tectonophysics* **282,** 277–289.

Istituto Nazionale di Geofisica e Vulcanologia
Sezione di Catania
Piazza Roma 2
95123 Catania, Italy
scarfi@ct.ingv.it; langer@ct.ingv.it
(L.S., H.L.)

Dipartimento di Scienze Geologiche
Università di Catania
Corso Italia 55
95129 Catania, Italy
gresta@unict.it
(S.G.)

Manuscript received 26 June 2002.